Simulation of Fluid Flow and Heat Transfer Process in Heat Exchangers in Petroleum Industries

Hardi Abdulla M. Rasul[1*], Mohammed Jawdat Barzanjy[2], Hazim Abed Mohammed Aljeware[3]

[1,2]*Chemical and Petrochemical Engineering Department, College of Engineering, Salahaddin University- Erbil, Erbil, 44001, Iraq; E-mail: hardi.m.rasul@su.edu.krd*

[3]*Petroleum Engineering Department, College of Engineering, Alkitab University, Iraq.*

Abstracts: Heat exchangers are very useful equipment in a wide range of industries, therefore the analysis of the internal flow in them is very important. In this study, a heat exchanger is modeled to solve the flow and temperature field. Three turbulence models have been tested for first and second order discretization using two different mesh densities, and the results are as follows. The effects of different parameters on the internal conditions of the converter have been simulated. The temperature changes decrease in proportion to the reduction of the heat transfer coefficient in viscous fluids, and the Reynolds number is greater than the Parantel number. For the tube with constant wall temperature and shell inlet, the heat transfer coefficient, pressure drop values and heat transfer rate are obtained. In another part, it is shown that the stabilization time of the fluid temperature has a direct relationship with the heat capacity of the pipes, and that the performance of the tubular heat exchanger with spiral walls is better than that of segmental walls. The intermittent temperature input has been investigated. It has been shown that the other flux will fluctuate with the same frequency, which it also proved our theoretical results.

Keywords: Tubular Heat Exchanger, Computational Fluid Dynamics, Boundary Conditions, Energy Conservation.

1. INTRODUCTION

Today, preventing energy-wasting is one of the important factors in the design and performance of the process industry. On the other hand, by reducing energy sources, energy resources prices are increasing every day, which provides competition over new designs and optimal use of resources. The design of optimal heat exchangers somewhat reduced costs and can have a significant impact on maintaining fuel resources. Therefore, the most important hydroelectric objectives are thermal performance and reduce the power of the pump [1-5]. The shell and tube type of heat exchangers are utilized in oil refineries and petrochemical industries classified Tubular Heat Exchanger (THE) for transferring heat between two fluids. These heat exchangers mostly have applications in preheating of the fluids[6-10].

Shell-tube heat exchangers are composed of tube, shell, front and rear heads, tube-sheet, nozzles and baffles[11]. These heat exchangers have some advantages such as the ability to apply in a wide range of temperatures and pressures, easy maintenance, include opening, examining, repairing, cleaning, and developing, in choosing the type of material used to make the heat exchanger, according to the problem of corrosion and other considerations, considerable flexibility and it can even be built out of different materials for shells and tubes, high contact level in low volume [12].

While, in the hydraulic section, the most important topic is the pressure drop of shells in the heat exchanger. The frequent drops of flow and contraction and expansion, and sudden changes in the flow pathway, increase the pressure drop in this type of heat exchanger. The vibration of the tube and sedimentation is also important in the operational problems. In fact, sedimentation and high levels of pressure drop can apply large costs to processes[13].

Computational fluid dynamics (CFD) is one of the advanced models and methods used for process control order to improve the complex systems and making the available for providing all the necessary input details[14]. High-reliable CFD simulations can be utilized to assess the existing performance, recover online control and assistance optimize operation of industrial processes[15]. Though, it should be noted that using CFD is often very challenging for simulation of large industrial processes and complex products owing to the existence of multiple scales for space and time in the industrial processes and the confines of the numerical techniques. Afrianto et al (2014) reported a numerical study on flow and heat transfer of a liquid natural gas in heat exchanger at 0.6 MPa. The CFD code FLUENT was utilized to simulate the fluids flow and heat transfer propertied in heat exchanger. The simulation was confirmed and paralleled with a reference one, representing effectiveness-NTU and LMTD method[16]. Hernandez-Parra et al

(2018) performed a CFD model under different operating circumstances for studying the production of non-aerated sorbet in a scraped surface heat exchanger. The modeling approach was reported to be consistent, as designated by contrasts between simulations of the heat transfers along the heat exchanger and experimental results[17]. Yu et al (2019) utilized CFD compressible model to analyze more accurate prediction models of heat exchanger performance. This study may provide some guidance to optimize the design of heat exchangers in order to save cost and energy[18]. Gurel et al (2020) made an evaluation for the thermo-hydraulic performance for a brazer PHE in order to develop and optimize the heat transfer and pressure drop of the PHE. The authors designed 3D lung like plate surfaces in order to increase the heat transfer area, then they run CFD simulations with Ansys-Fluent program in operating condition (under 90 °C and 40 °C and the flow of 0.05 kg/s). Quite irregular fluid velocity in plate cavities was observed due to the formation of turbulence at constant Reynolds numbers which elaborated its effectiveness[19]. Hanan et al (2021) investigated a heat exchanger utilizing CFD. The results exposed that inlet velocity decrease, thermal conductivity increase, baffle spacing reduction and triangular tube bundle arrangement was significantly affect the reduction of the condensate temperature[20].

In conventional methods of CFD, the numerical evaluations are discretized by means of mesh elements, entirely depend on the mesh quality and the features of involved phenomena such as physical, chemical and mechanical properties. The features of microscale (e.g. boiling) and macroscale (such as burners) in industrial processes is very difficult to make a suitable mesh and perform simulation in a proper timeframe for the results to be used in the steps of design or in online control[21]. However, these limitations could not overcome the use of CFD for heat transfer and fluid flow simulations. A good option is to make simpler the geometry of the process by smearing appropriate boundary circumstances, and simulate a small section of the process to get a precise solution[22]. Kanaris et al (2006) explore the potential use of the general purpose CFD code to figure the properties of the flow field, and of the heat transfer augmentation in conduits with corrugated walls in commercial plate heat exchangers (PHE). It was illustrated that CFD code is an actual and consistent way of studying the influence of various geometrical configurations on the optimum design of a PHE[23]. The developing utilize of SPHydro completely different designing CFD applications within the final two decades clearly indicates its potential within the field of CFD[24, 25]. In any case, since of the straightforwardness of the SPHydro calculations, it is simple to parallelize the code to attain significant speed-up by utilizing HPC offices architecture-based parallel clusters. This is often why SPHydro is heavily utilized in computer illustrations businesses for visualization of the extraordinary liquid streams and heat impacts in movies and recreations[26, 27].

Then, the overall objective of this study is to perform high faithfulness fluid flow and heat transfer simulations for petroleum industrial process for better understanding the energy-related processes and to investigate the products numerically in detail using CFD method in commercial packages, and highpoint the limitations and challenges. Then, we aimed to to use CFD to elucidate energy-related oil industrial processes, where flow and heat transfer issues are serious. The petroleum refinery application studied in this thesis is heat exchanger optimization. The studied problem covers multi-phase flows. The case also covers heat transfer in the form of conduction and convection. However, the observations exemplified in this thesis may serve as a decision instrument to choice a suitable CFD tactic to deal with this type of industrial issues.

2. MATERIEL AND METHODS

2.1. Simulation of thermal behavior of the heat exchanger

As mentioned, there are many methods for analyzing the flow in heat exchangers, most of these methods are based on steady state conditions and do not have the ability to predict the dynamic characteristics of the exchangers. If there are many issues in the industry that need to be properly dealt with, consider the unstable conditions of the converter in the designs. Many factors can cause a dynamic situation or time function (unstable). For example, a change in the input conditions of one of the hot and cold streams, such as flow rate, temperature, physical properties or changes in the environmental conditions of the converter, etc., are all among the factors that can cause an unstable state. In the presented model, the converter consists of four components: inner duct, inner wall, outer duct, and outer wall. The side view of the converter is shown in Figure 1. In Table 1, the geometric characteristics of the converter are

shown.

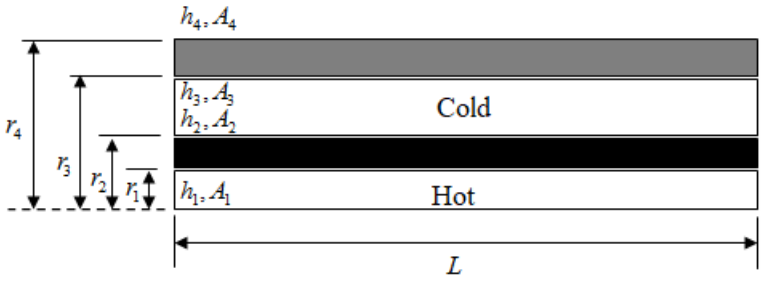

Figure 1. Different areas of numerical analysis.

Table 1. Geometric specifications of the heat exchanger

Shell inlet diameter	$345.87mm$
Shell Thickness	$10mm$
Length of the shell	$4230mm$
Tube inlet diameter	$16.3mm$
Tube Thickness	$1.22mm$
Length of the Tube	$3865mm$
Tube Pitch	$19.66mm$
Transverse Pitch	$17.23mm$
Baffle Cut	$25\%d$
Baffle Number	15
Tube sheet Number	2

2.2. Basic Consideration

The basis of the simulation work is to provide a suitable mathematical model. In this regard, a method known as the limited volume method is used. The domain of analysis includes four sections: flow and tube wall, flow and loose wall. Each of these parts is divided into n+1 parts, then energy balance is applied to each of these volume components that form a control volume.

2.3. Heat transfer mechanisms

For fluid control volume, heat transfer is done by the method of forced displacement and heat transfer caused by the mass movement of the fluid. Heat conduction in the axial direction inside the jet is ignored due to its small size compared to the mentioned cases. In solid walls, these mechanisms include forced displacement and axial conduction. The subject of guidance inside the walls is a subject that has been neglected in most of the previous works. In both cases, the flow and the wall, due to the unsteadiness of the analysis, the derivatives of temperature with respect to time appear in the equations.

2.4. Boundary conditions

The boundary conditions for the fluxes appear in the form of known values in the equations. Of course, insulation boundary conditions are considered for the walls. For this purpose, for the heat conduction of the two volume components of the beginning and the end, respectively, only the output and the input have been considered, and based on this, the equations related to these volume components have been obtained separately. In fluxes, the inlet boundary condition of fixed temperature is adopted. Therefore, the same equation as other volume components

cannot be considered for the input volume components in the fluxes. This is why the number of equations for each of the fluxes is one less than for the walls. For each of the walls, the number of volume components, i.e. n+1 equations, and for each of the fluxes, one less equation is obtained, i.e. n equations. According to the four components in the heat exchanger (internal and external fluxes and internal and external walls) and according to the above content, there will be a total of 4n+2 first order differential equations for each time step.

The temperature in the radial direction is uniform and the same in each section of the volumetric component. But in the distance between two nodes, different profiles for temperature can be considered, the simplest of which is the linear profile. The type of selection of nodes inside each volumetric component is based on the central cell method. In this situation, for more accuracy, the first and last volume components have a length equal to half of the other volume components. For this reason, a difference has been created between the equations obtained for this volume component and other volume components.

The workflow for each domain of analysis starts with providing a sample view of a volume component within the domain. In this plan, all the input and output heat fluxes are given to the volumetric component. Then, by applying the energy balance for the volume component, the relationship between the temperature changes with respect to time and the input and output fluxes has been obtained. In the equations, relations such as Fourier's relation and Newton's law of cooling are used to communicate between heat fluxes and node temperatures.

2.5. Expansion of spatial derivatives

The next step is to expand the spatial derivatives of temperature. It is possible to expand the derivative of functions in differential form in different ways. Basically, theoretically, in this method, the values of the dependent variable are calculated at a number of points of the solution domain (so-called nodes) by focusing attention on the values in the nodes, the continuous information obtained from the exact solution of the differential equation. It turns out that their origin is reference differential equations.

The obtained equations are differential or discontinuous equations. Meanwhile, the computational field is divided into a number of smaller fields and a separate profile for the investigated function will be created on each of these subfields. In this way, the differential equations will be replaced with simple algebraic equations that have a much simpler solution and the calculations will be much easier. Considering the above, in the continuation of the mathematical modeling of spatial derivatives obtained will be written differentially. Using this method, the equations of partial derivatives are simplified and finally what remains will be the first order differential equations.

Spatial derivatives of the obtained equations are written differentially, considering that the domain of solution is divided into elements using the existing differential formulas, which are based on Taylor's expansion. The type of differential formula used (progressive or central regressive) is selected according to the position of the element. For example, central differential, which is more accurate, is used to conduct heat inside the walls in the middle points, but progressive and backward differential are used for the beginning and end elements, respectively.

These changes in the type of difference used depend on the presence or absence of previous and subsequent temperatures in the desired volume component. The next step is to arrange the equations, so that on the left side of the time derivative of the temperature of the corresponding volume component, and on the right side of the equation, there are coefficients of the temperature of the relevant domain and other domains. In total, there will be 4n+2 equations and the same number of unknowns that include the different temperatures of the jets and walls. The known values in the equations are the inlet temperature of the hot fluid, the inlet temperature of the cold fluid and the temperature of the surrounding environment. It should be noted that displacement with the environment is also considered for the external wall, which will make the problem more comprehensive. At the same time, it is easy to reduce or increase the inputs of the problem by considering different boundary conditions. In the past works, the heat exchanger is usually considered as insulation.

2.6. Applying energy conservation

In the following, equations are obtained for each volume component based on the conservation of thermal energy. In general, the assumptions used to obtain the following equations can be summarized as follows.

1) Temperature is only a function of x and t.

2) The system has heat exchange with the surrounding environment by displacement method (free and forced). But the heat transfer on the sides of the converter is zero.

3) There is no heat conduction in the x-longitudinal direction in the jets, but inside the walls there is heat transfer in the longitudinal direction by conduction method.

4) The heat capacity, conductive heat transfer coefficient, flux density and also the heat transfer coefficient inside the ducts are constant.

5) The temperature and properties of the fluid and brain building material in each volume component are considered uniformly.

6) The fluid of the internal pipes is cold and with the subscript (c) and the fluid passing through the outer part of the tubes (shell) is considered the hot fluid with the subscript (h). When it is hot or cold, there is no fluid passing through any of the ducts.

Analytical domains of hot flow, cold flow, internal walls and external wall are considered as volumes and energy conservation is applied for each of them. The result is to obtain several sets of differential equations, each of which is related to a field of analysis. The expansion of equations is written in S file.

3. RESULTS AND DISCUSSION

In the previous section, how to obtain state, input, output and transition matrices was specified. Now, by using the organized software set, it is possible to simulate different working conditions for the shell and tube converter. In this section, the conditions caused by some changes in geometry, flow and environmental conditions have been investigated. Then, the effect of changes in mass flow rate, heat transfer coefficient of the external environment of the converter, the type of fluids and the type of pipes on the stable and unstable state of the converter is investigated. Application of stepped and alternating temperature inputs and evaluation of converter response is another part of this series. Finally, a comparison has been made between the data obtained from the simulation and the numerical data.

Table 2. Physical and geometric parameters of the heat exchanger in project mode.

	Tube	Shell
Fluid	Water	Oil
Material	Cupro – Nickel = $\frac{55}{45}$	C.S
$k\left[\frac{watt}{m.k^{\circ}}\right]$	23	60.5
$cp\left[\frac{J}{kg.k^{\circ}}\right]$	384	434
$\rho\left[\frac{kg}{m^3}\right]$	8920	7854

Table 3. Geometric specifications of the heat exchanger.

Shell inlet diameter	$345.87mm$
Shell Thickness	$10mm$
Length of the shell	$4230mm$
Tube inlet diameter	$16.3mm$
Tube Thickness	$1.22mm$
Length of the Tube	$3865mm$
Tube Pitch	$19.66mm$
Transverse Pitch	$17.23mm$
Baffle Cut	$25\%d$
Baffle Number	15
Tube sheet Number	2
baffle spacing and helical pitch	$22mm$

Table 4. Boundary conditions.

Boundary	Boundary Type	Values
Inlet shell	Mass flow inlet	0.50 - 2.00 kg/s & 25 c0
Outlet shell	Pressure outlet	0 Pa (Gauge pr.)
Inlet tube	Mass flow inlet	0.5 kg/s and 55 C0
Outlet tube	Pressure outlet	0 Pa (Gauge pr.)
Shell wall	Wall, Stationary, no slip, adiabatic	Adiabatic
FRP Baffle	Wall	Conducting
Domain inside shell	Fluid	------
Domain inside tube	Fluid	------
Domain of baffles	Wall	------

As mentioned in the previous section, the displacement heat transfer coefficients inside the tube are obtained using Sider's and Tate's formula (File S), for three different regimes of laminar, transitional and turbulent flow. And for the displacement heat transfer coefficient on the shell or shell side, equations in File S has been used. Also, for the external heat transfer coefficients in the free displacement mode, the equations (File S) of Chechil and Chu have been used. Geometrical and physical conditions are similar in most cases and are according to Table 5. The inner tube material is cupro-nickel 45-55 and the shell material is carbon steel. Generally, these conditions are constant unless there are changes in the material and geometry. In this case, they will be mentioned in the relevant sections. In all the converters that are examined, the cold fluid flows in the inner duct or the pipe and the hot fluid flows in the outer duct or the shell. But as it has been said in the previous sections, there is no restriction on the fluid being hot or cold in any of the ducts, and this was done only for greater coordination in the work.

In the graphs, t is the time and its unit is seconds, x is the distance from the beginning of the converter, and L is the length of the converter. T is the temperature of different points in the desired converter, and its position is determined by the indices w_{out}, w_{in}, c, h, which respectively correspond to the hot fluid; cold fluid; The inner wall and the outer wall. $T_{h_{in}}$ is the inlet temperature of the hot fluid and tc_{in} is the inlet temperatures of the cold fluid. in Figure 2, a view of heat exchanger and baffle meshing with mesh number 1,359,855 is shown.

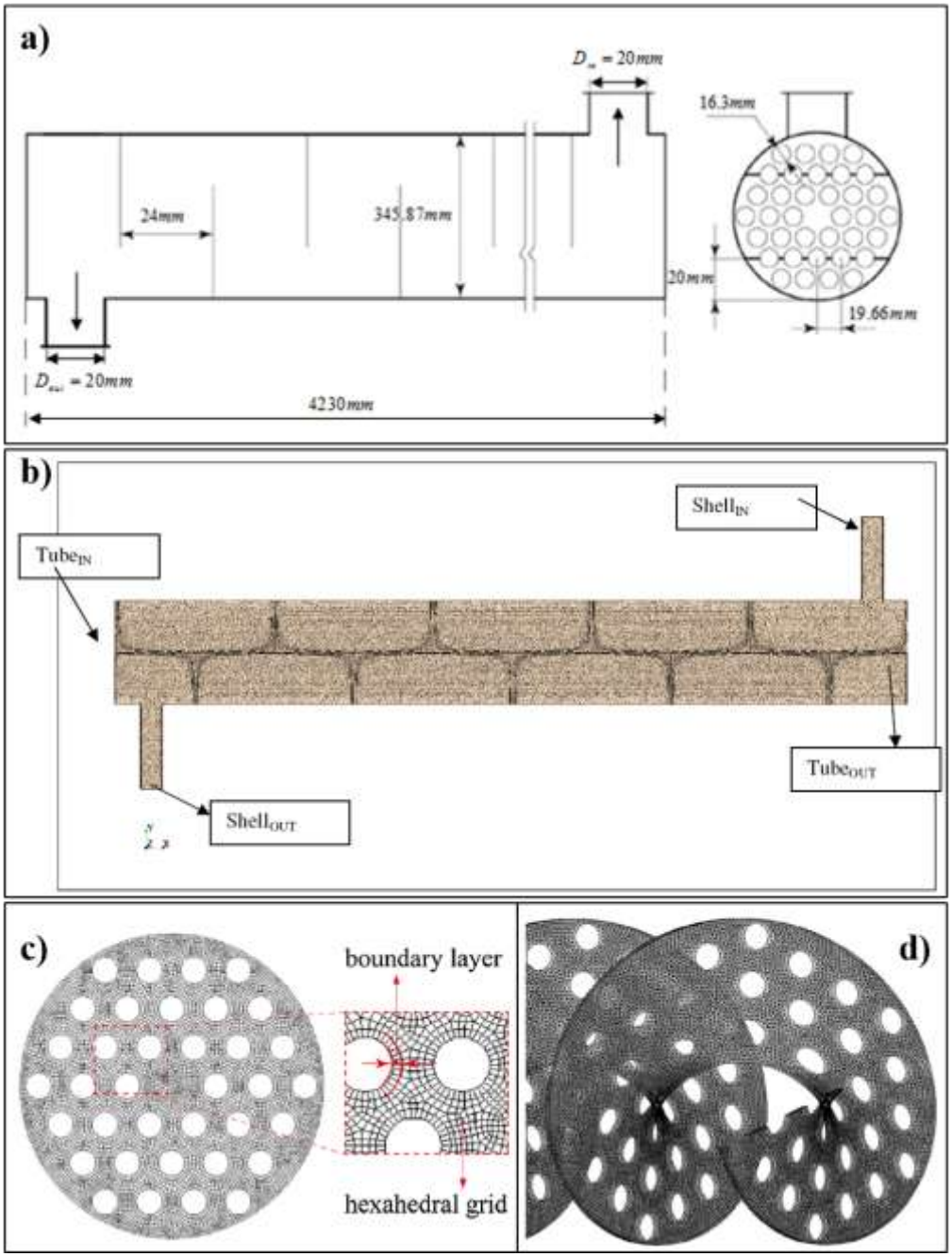

Figure 2. Schematic illustration of shell-tube heat exchanger (a); networking of shell-tube heat exchanger (b); networking of the shell-tube heat exchanger from the side view for the passing plate of the tube (c); and networking for the shell-tube heat exchanger from the side view for the baffle (d).

The scope of calculations according to Figure 2 a and b, using an unorganized style for the central area and a two grid structure for the entrance and border and exit areas, has been done using spatial discretization. In order to be independent of the network, four networks with different dimensions are given in Table 5, they are used and the outlet temperature and pressure drop for different networks are compared. The results show that the biggest difference between the results of the two recent networks is less than 0.000632%, so that the network with the size of 1,035,570 cells has been used for simulation in this thesis. Independence from the network is done according to the highest value of the Reynolds number. Also, experimental data for shell-and-tube heat exchanger, has been used to validate the computational code.

Table 5. Mesh numbers for independence from the network with Pr=14,55 and Re=3300 for fluid.

Mesh	M1	M2	M3	M4
Number of nodes	656230	795852	998421	1,245,066
Number of elements	674899	801257	1,035,570	1,359,855
Cold Outlet (K)	325.63	326.95	328.67	328.85
Hot Outlet (K)	342.15	343.86	344.77	344.80
Nu_{ave}	32.652	35.120	36.548	36.548

The Nusselt number scale is approximately five decimal places. Therefore, a grid size of 1,359,855 elements is determined based on the Nusselt number data to satisfy the independence of the grid. In our Fortran numerical simulation, 1,035,570 is the most optimal number of elements.

3.1. Effect of step changes in flow rate

In this section, the effect of step changes in the flow rate of two jets on the outlet temperature of the jets and the average temperature of the walls has been investigated. The analysis results are shown below. In the graphs, a parameter appears in the form that is defined as follows:

$$\boldsymbol{\gamma_{h/c}} = \frac{\boldsymbol{m_{h/c}^{\dot{}}}}{\boldsymbol{m_{h/c}^{\dot{ref}}}} (1)$$

Here, $m_{h/c}^{\cdot}$ is the value of the mass flow in the new state and $m_{h/c}^{\dot{ref}}$ is the mass flow in the initial or reference state. The initial mass flow of the hot fluid is 200 kg/s and the mass flow of the cold fluid is 244.8 kg/s, at the beginning. The cold fluid is water and the hot fluid is oil. Changes in the flow rate have been made as a doubling of the initial values. The geometrical and physical characteristics of the converter are given in Table 5, which are constant during changes. The flow characteristics of the fluxes are also shown in Table 6.

Table6. Flow specification for step change in flow rate.

Sample time) S(	$\dot{m}_h \left[\frac{kg}{\sec}\right]$	$\dot{m}_c \left[\frac{kg}{\sec}\right]$	$Th_i \left(c^\circ\right)$	$tc_i \left(c^\circ\right)$	Type of flow arrangement
30	Dynamic	Dynamic	100	20	same direction

Figure 3 shows the effect of changes in the mass flow of hot and cold fluids on the hot outlet temperature.

Figure 3a shows the effect of changes in the mass flow rate of two jets on the temperature profile of the hot jet at the outlet. According to Figure 3a, it is clear that with the increase in the mass flow rate of the hot fluid, the temperature of the hot fluid at the outlet increases and with the increase in the flow rate of the cold fluid, the temperature of the hot fluid decreases, which is obvious. Increasing and decreasing the cold flow rate increases and decreases the cold flow rate, respectively, and the highest temperature of the hot fluid is related to the increase of the hot fluid flow rate. Dynamically, it is clear that the stability time for the hot fluid increases with the increase in the ratio of the flow rate of the cold fluid to the hot fluid.

Figure 3b shows the effect of changes in the mass flow rate of two jets on the temperature profile of the cold jet at the outlet. According to Figure 3b, the temperature of the cold stream has an inverse relationship with the rate of cold mass flow. That is, as it decreases, it increases and as it increases, it decreases. At the same time, this temperature has a direct relationship with the flow rate of hot fluid. In a situation where the only change is an increase in the hot mass flow rate, the temperature of the cold fluid occupies the highest value, and at the same time, the stability time of the cold fluid also increases. But in a situation where both the flow rate of the cold fluid and the flow rate of the hot fluid increase step by step, an intermediate state occurs. The lowest temperature is also for the cold fluid when the flow rate of the cold fluid increases alone. The lowest speed of stability is related to the state where the hot flow rate is doubled and the cold flow rate remains constant.

Figure 3c shows the temperature profile of the inner wall section (tube) over time for changes in the mass flow rate of hot and cold fluids. We can see the effect of changes in the mass flow rate on the wall temperature. In general, the temperature of the walls is affected by the temperature of the fluids around it. For the inner wall, the temperature is in a range between the temperature of the hot fluid and the temperature of the cold fluid, but in this figure, it seems that the temperature of the inner wall is more affected by the temperature of the hot fluid. When the mass flow rate of the hot fluid increases, the wall temperature also increases. This issue happens oppositely in the conditions of changes in the flow rate of the cold fluid. When the flow rate of the hot fluid increases, the rate of stabilization of the average temperature profile of the inner wall also decreases. Also, the simultaneous doubling of hot and cold fluid flow does not have much effect on the temperature of the inner wall. Figure 3d shows the temperature profile of the middle section of the outer wall (shell) over time for changes in the mass flow rate of the two jets.

Similar conditions exist in the outer wall, with the difference that in this case the temperature of the wall is strongly affected by the hot flux. As the mass flow rate of the cold fluid increases, the temperature of the outer wall decreases and as the hot flow rate increases, the temperature of the outer wall increases. Due to the insulation of the external surface of the shell, the temperature of the shell increases despite the stabilization of the flow in the fluxes and the tube.

In this way, it can be said that by increasing the mass flow rate of hot fluid, the temperature of different areas increases and by increasing the flow rate of cold fluid, the temperature of different areas decreases.

3.2. Changes in the heat transfer coefficient, displacement of the environment and its effect on the efficiency of the converter.

The environmental conditions of the heat exchanger can have different changes. In this case, the heat transfer coefficient outside the exchanger has different values. In this section, it is assumed that the surrounding environment of the converter is surrounded by air. But in general, you can choose any gender for the surrounding environment. According to the condition of insulation and two mechanisms of heat transfer with the environment and taking into considerations (File S), three values for the coefficient of heat transfer with the environment have been considered. The first condition is h=0, which indicates the condition of insulation of the transducer, h=3.6, which indicates the condition of free movement, and h=30.7, which corresponds to the forced movement of the transducer with the environment in a forced state. The characteristics of the current inside the converter are given in Table 7.

Table7. Flow characteristics for different heat transfer coefficient of the surrounding environment, changing the type of

fluxes, and different types of pipes.

Sample Time (S)	$\dot{m}_h \left[\frac{kg}{\sec}\right]$	$\dot{m}_c \left[\frac{kg}{\sec}\right]$	$Th_i\left(c^\circ\right)$	$tc_i\left(c^\circ\right)$	Type of flow arrangement
30	200	244.8	100	20	same direction

The geometric specifications of the converter are given in Table 5.

Figure 3e shows the time profile of the outlet temperature of the hot fluid for different values of the heat transfer coefficient of the ambient displacement. According to the shape, the maximum temperature of the hot fluid outlet is related to the insulation state. As the value of the heat transfer coefficient of the environment increases, the amount of heat loss from the surfaces of the converter increases. This causes a decrease in temperatures, including the outlet temperature of the hot fluid, and generally lowers the heat and temperature efficiency of the converter. Since the temperatures are in the lower range, the changes made in the temperature profiles of Figure 3e are not very noticeable. But in conditions where higher temperatures are considered inside the exchanger, the effects of changing the displacement heat transfer coefficient will be greater.

3.3. Changing the fluid type and its effects

Another thing that has been taken into consideration is the choice of different genders for the fountain. Here, obviously, different types of hot fluid are considered. For this purpose, three types of oil, diesel and gasoline are considered. In this condition, the material of the cold fluid flowing in the tube is constant (water). The geometric specifications of the converter are listed in Table 5 and the flow specifications are listed in Table 7.

Figure 3f shows the temperature profile of the cold fluid, which is water, in exchange for time changes for three types of hot fluid. The temperature profile of the cold fluid reaches a steady state more slowly for the case where the hot fluid is gasoline. This issue can have two reasons, firstly, the heat capacity of gasoline is higher than the other two types. Therefore, its thermal inertia is higher and it reaches a stable state more slowly. In this condition, the hot fluid (gasoline) will surely reach stability more slowly than other conditions (Figure 3g).

The second issue is the high heat transfer rate. According to the properties of the desired fluids, the highest viscosity is related to oil and the lowest viscosity is assigned to gasoline. In similar conditions of speed and geometry based on Equation of File S, the highest heat transfer is related to gasoline and the lowest is related to oil. Temperature changes in oil are less than gasoline, which is due to the high heat transfer coefficient of gasoline. Although the Parantel number of oil is much larger than that of gasoline and diesel, the effect of the Reynolds number (which is higher in diesel and gasoline than oil) is much greater. This will increase the transfer of heat from the hot fluid (gasoline and gasoline) to the cold fluid (water). The minimum temperature changes of the cold fluid are also due to the minimum heat transfer for the oil type (as a hot fluid). The lowest stabilization time of the hot and cold fluid profile is related to the type of oil and the longest time is related to the type of gasoline. The reason for this, as mentioned above, is the lower heat capacity and the lower Reynolds number, and as a result, the lower heat transfers for the oil type compared to the others. Therefore, it can be concluded that the heat transfer inside the converter is directly proportional to the Reynolds number and the Prantel number, but the Reynolds number is much more effective.

3.4. The effect of pipe material on dynamic parameters

The pipes used in the heat exchanger structure can be selected from different materials. As previously mentioned, the characteristics given in Table 5 for internal and external pipes are respectively related to COPRO-NICKLE 55/45. In this section, the effect of different types of pipes has been investigated. Figures 3h and 3i show the effect of the type of inner tubes for the dynamic and static characteristics of hot and cold fluids. In this case, four types of inner tubes are considered. These four types are STEEL, BRASS, COPPER and COPRO-NICKLE 55/45; flow

specifications are given in Table 7 and converter geometry specifications are given in Table 5. The internal fluid is made of water and the external fluid is made of oil.

In all four cases, all other specifications, such as flow rate, type of fluxes, duct sizes, thicknesses, etc., are similar, and only changes are made in the material of the inner pipe. According to Figure 3h, in the case where the inner tube is made of BRASS and COPPER, compared to the other two cases, the temperature profile of the hot fluid at the outlet reaches stability later.

The same situation is observed in cold fluid (Figure 3i). That is, in this case, the temperature profile of the cold fluid for BRASS and COPPER pipes has a phase delay compared to the other two cases. The reason for this should be found in the difference between the heat capacity of these two pipes and other cases.

In these two cases, the heat capacity is much higher than the other two cases, i.e. the type of pipe - COPRO 55/45 NICKLE and STEEL. Therefore, more heat is used to change the temperature of the inner wall in these two genders. In this situation, the hot and cold temperature profile has a time delay compared to other types of pipes. Of course, in terms of the steady state, the temperature of the fluxes also decreases in the case of copper and steel pipes.

Therefore, it can be said that with the increase in the thermal inertia of the walls, which can be caused by changes in their material, the stability time in all the components of the converter increases and the thermal efficiency of the converter decreases.

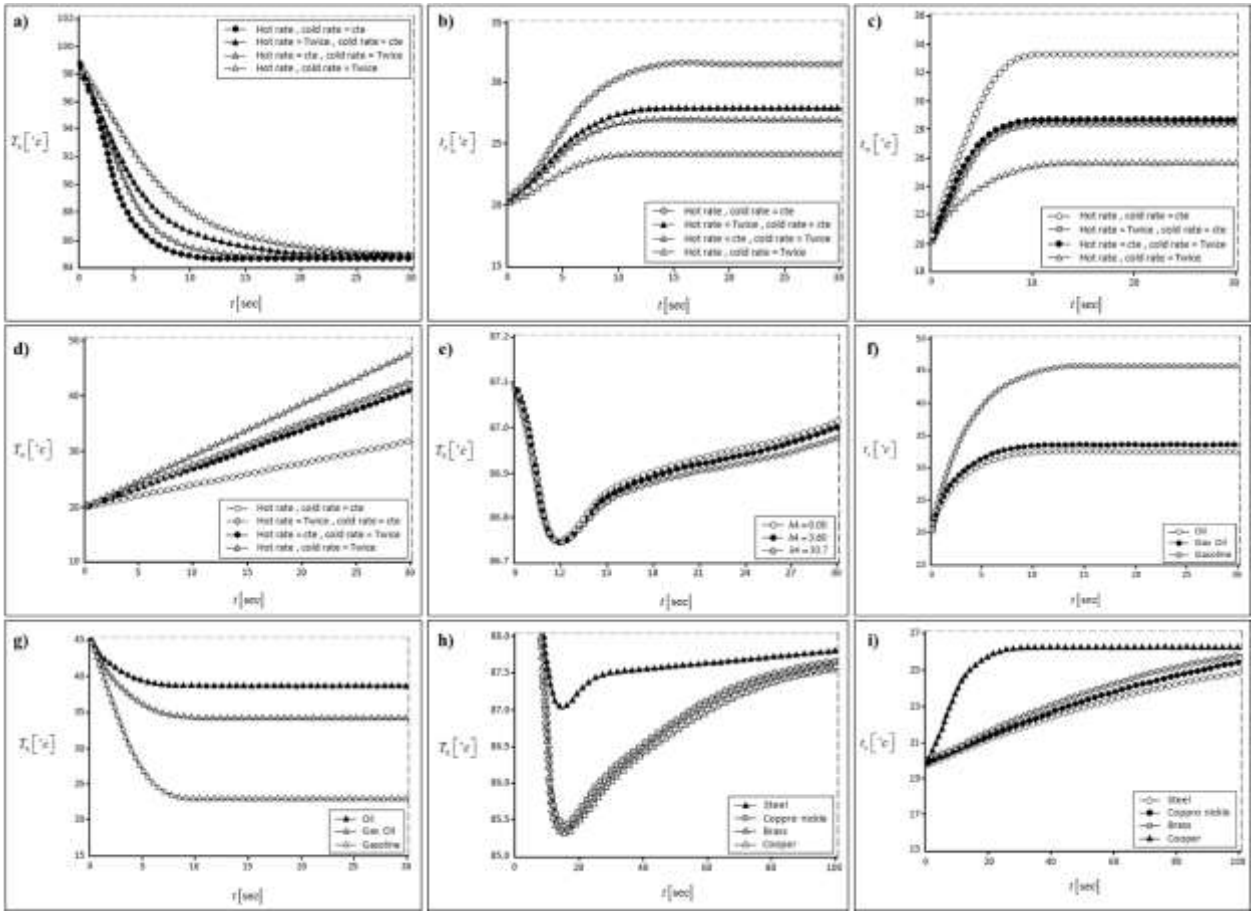

Figure 3. The outlet temperature of hot fluid (a) and cold fluid (b) in terms of time for different mass rates of cold and hot fluids; middle part temperature of inner wall (c) and outer wall (d) of the tube in terms of time for different mass rates of cold and hot fluids; outlet temperature of hot fluid in terms of time for different hours (e); outlet temperature of cold fluid (f) and hot fluid (g) in terms of time for different types of hot fluid; outlet temperature of hot fluid (h) and cold fluid (i) in terms of time for different types of internal pipe.

3.5. Simulation diagrams of co-directional flow in steady state

In this section, the dynamic and static analysis of the co-directional flow arrangement is discussed. The geometry of the converter is based on the items mentioned in Table 5. The current characteristics are given in Table 7. These items are fixed in all the simulations related to this section.

In this case, the cold fluid passes through the tubes and the hot fluid passes through the shell, and the fluid inside the tube is water and the fluid inside the shell is oil. The graphs obtained in simulating the co-directional flow arrangement are given below.

3.5.1. The temperature of different points of the filed according to location at different times

Figure 4a is related to the graph of changes in the temperature of the hot fluid relative to the location at different times. The inlet temperature of the hot fluid is constant, which is at the beginning of the converter for the flow in the same direction. For the initial points and close to the inlet, the temperature changes very quickly, so that at the moment s t = 6, the temperature of the initial points to the center of the converter is in an acceptable range in terms of stability. But with the passage of time and the transfer of heat from the hot fluid to the cold fluid, the temperature of the hot fluid starts to decrease towards the end of the converter, and in the steady state, the temperature profile of the hot fluid assumes an almost linear shape.

The temperature profile at different points of the cold stream at some specific times for the co-directional flow arrangement is given in Figure 4b.

The drawn lines show the cold fluid temperature profiles at different times. Due to the juxtaposition of hot and cold inlets in the co-directional arrangement, the temperature of the initial points increases at the very beginning. This is evident in the profile corresponding to s t=4. With the passage of time, the temperature of the points to the end points of the cold stream, the temperature of the cold stream in this section also increases. From the moment s t = 10 seconds onwards, the drop of the temperature profile of the cold fluid at the end of the converter has almost disappeared and the overall shape of the profile approaches the stable state, i.e. linear. Figure (4c) shows the temperature changes of the tubes according to location at different times. As it can be seen, the temperature of the tube at x=0 is almost constant due to the lack of heat transfer for all diagrams, but with the passage of time and during the converter, the temperature of the tube starts to increase and at time t=30 s, it almost reaches the state It becomes stable and the temperature of the tube takes a linear shape.

Figure (4d) shows the graph of the included temperature changes by location at different times. In the early times, its temperature is almost constant along the entire length, but with the passage of time, the shell temperature increases. With the passage of time and due to the transfer of heat from the hot fluid to the cold fluid, the shell temperature takes a linear shape and decreases slightly along the length and in the direction of the hot flow.

In this section, the temperature profiles obtained for different points of the converter in terms of time in the same direction flow have been investigated.

Figure (4e) shows the temperature changes of the cold fluid at the inlet and outlet in terms of time. As it is evident from the graph, the temperature of the cold fluid inlet point does not change much due to the same direction of the hot and cold fluid, but the temperature of the cold fluid outlet point starts to increase very quickly and after t=15 seconds, it reaches the state It arrives stable.

Figure (4f) shows the temperature changes of the hot fluid at the inlet and outlet in terms of time. When the hot fluid enters the converter with a temperature of 100 °C, due to the small distance from the beginning of the converter, a little heat transfer is done with the cold fluid, and as a result, the temperature of the hot fluid at the inlet drops less. At the outlet of the converter, due to the same direction of the hot and cold fluid and having enough time for heat transfer, the temperature of the hot fluid starts to decrease from the very beginning until it reaches stability around t=12 s.

Figure (4g) shows the temperature changes of hot and cold fluid according to location at time t=30s. As it is evident from the figure, during the stability time, the temperature of the cold fluid increases linearly and the temperature of the hot fluid decreases linearly. The temperatures shown in this diagram are related to the steady state of the converter.

3.5.2. Temperature Response of the Converter to Step Input

As it was said before, by using modeling using the state space method, it is possible to create a great variety in the temperature input. This variety includes all inputs including the temperature of the hot and cold fluid and the temperature of the air near the converter. This means that no additional calculations are added to the calculation volume. Therefore, in a short time, all types of inputs to the system can be tested.

a) The inlet temperature of the cold stream in the form of a step

The geometric characteristics of the converter are the same as those mentioned in Table 5 and the current characteristics are as follows. The internal fluid is water and the external fluid is oil, and the flow characteristics are listed in Table 7.

Figure (4h) shows the cold fluid temperature change graph by location at different times for the step function of the cold fluid. As it is evident from the figure, with a step change in the temperature of the cold fluid from 20 to 10, in the early times, the shock created in the temperature of the cold fluid did not spread in the length, but with the passage of time, the shock created in the length spread and the temperature of the cold fluid decreased. And at time t=30s, it has almost assumed a linear shape and reached a stable state.

Figure (4i) is the graph of cold fluid temperature changes in terms of time at the beginning and end of the converter. The geometric characteristics are the specifications of Table 1 and the flow characteristics are the same as those of Table 7 with a step change in the temperature of the cold fluid from 20 to 10 at the beginning of the temperature converter, the temperature is immediately affected and reduced, but due to the transfer The heat from the hot fluid to the cold fluid reaches a value greater than 10, and at the end of the converter, it takes some time for the disturbance created in the cold fluid to reach the end of the converter, and the slope of temperature changes at the outlet is much milder than the slope of temperature changes at the inlet section. . Finally, the temperature of the cold fluid at the outlet reaches a stable state at time t=20s, but due to heat transfer from the hot fluid to the cold fluid, its temperature becomes higher than the inlet temperature.

Figure (4j) shows the graph of hot fluid temperature changes over time at the inlet and outlet of the converter for a step change in cold fluid temperature. The geometric specifications are the specifications of Table 5 and the flow specifications are the same specifications of Table 7. With a step change in the temperature of the cold fluid from 20 to 10, the temperature of the hot fluid at the beginning of the converter does not change much due to lack of opportunity for heat transfer, in other words, a step change in the temperature of the hot fluid is not felt at the entrance of the converter. While at the end of the converter, the disturbance created in the temperature of the cold fluid increases the heat transfer from the hot fluid to the cold fluid and decreases the temperature of the hot fluid.

Figure (4k) shows the change of shell temperature according to location in the previous state. As it is evident from the graph (k), the disturbance created in the temperature of the cold fluid causes the temperature of the shell to decrease along the length of the converter, but due to the transfer of heat from the hot fluid to the shell and the insulation of its outer wall, with the passage of time the temperature of the shell in Each point increases.

Figure (4l) is the graph of cold fluid temperature changes according to location at different times for step change of hot fluid temperature from 100 to 145. The geometric specifications are the same as the specifications in Table 1 and the flow specifications are according to Table 8. As the temperature of the hot fluid increases step by step, the temperature of the cold fluid also increases along the length of the converter. This temperature change is more noticeable in sections close to the outlet of the converter. In the initial times, the disturbance created in the hot fluid has not yet reached the end of the cold fluid and the temperature of the end points has not changed much, but with

the passage of time, the disturbance created in the hot fluid causes more heat to be transferred to the cold fluid and the temperature of the end points of the cold fluid increases. In steady state, the temperature graph is linear.

Figure (4m) shows the graph of hot fluid temperature changes in terms of time at the beginning and end of the converter for the step function of hot fluid temperature. The geometric specifications are the same as the specifications in Table 5 and the flow specifications are according to Table 8. As can be seen from the figure, the change in the temperature of the hot fluid at the beginning of the converter has an immediate effect and causes an increase in the temperature of the hot fluid at the beginning of the converter, but it takes some time for the disturbance created at the beginning of the hot fluid to reach its end. But due to the heat transfer with the cold fluid, the temperature of the hot fluid at the outlet is less than 145 with the passage of time and it takes approximately t=20 s for this disturbance to reach a stable state.

Figure (4n) is the graph of cold fluid temperature changes in terms of time at the beginning and end of the converter for the step function of hot fluid temperature. The geometric specifications are the same as those in Table 5 and the flow specifications are according to Table 8. As it is evident from the figure, the step change created in the temperature of the hot fluid during the initial period of the cold fluid does not have much effect on time, but at the end of the converter, the temperature of the cold fluid increases over time and after about t=20 s it becomes It arrives stable. The reason for the increase in the temperature of the cold fluid is the increase in heat transfer from the hot fluid to the cold fluid due to the increase in the temperature of the hot fluid.

Figure (4o) is the diagram of shell temperature changes according to location at different times for the step function of hot fluid. As can be seen from the graphs, as the temperature of the hot fluid increases, the shell temperature increases with time along the exchanger. This increase in temperature reaches a stable and linear state at time t=30 s.

3.5.3. Temperature Response Of The Converter To Intermittent Input Temperature

As mentioned before, by using state space modeling, it is possible to create a large variation in the inlet temperature. This variety includes all inputs including the temperature of the hot and cold fluid and the temperature of the air near the converter. This means that no additional calculations are added to the calculation volume. Therefore, it is possible to test all kinds of inputs to the system in a short time. One of the inputs that can be useful is the alternating input. In this section, a sinusoidal input is considered for the hot fluid temperature. The geometric specifications of the converter are the same as mentioned in Table 5 and the current specifications are as follows. The cold fluid is water and the hot fluid is oil.

Table8. Current specifications for the step function of hot fluid temperature.

Time Sample (S)	$\dot{m}_h\left[\frac{kg}{\sec}\right]$	$\dot{m}_c\left[\frac{kg}{\sec}\right]$	$Th_i\left(c^\circ\right)$	$tc_i\left(c^\circ\right)$	Type of flow arrangement
270	200	244.8	$100+10\sin(t)$	20	same direction

3.5.4. Sinusoidal hot fluid inlet temperature

According to the Table 8, the temperature of the hot fluid entering the system is sinusoidal with a range of 10 degrees Celsius and a base value of 100 degrees. Figure (4p) shows the temperature profile of the hot fluid inlet and outlet over time. In this image, two alternating profiles are given, one is related to the inlet temperature and the other is the outlet temperature of the hot fluid. In this case, the inlet temperature of the hot fluid is considered as an input disturbance to the system. According to the figure, it is clear that the outlet temperature range is smaller than the inlet temperature range. The hot fluid temperature at the outlet has a phase delay compared to the input disturbances. This delay is about 5 to 7 seconds. The distance between two consecutive maxima in the inlet and outlet temperature profile is equal, which indicates that the frequency at the inlet and the outlet response are constant.

Figure (4q) shows the temperature changes of the hot fluid in terms of time at the entrance and exit for the sinusoidal function of the fluid. The cold fluid undergoes a sinusoidal change $20+5\sin(t)$ and as it is clear from the figure, the temperature of the hot fluid at the outlet receives disturbances with a time delay of 8 seconds and undergoes an oscillating change with the same frequency but with a smaller range of changes.

3.5.5. Checking The Number Of Points In Steady Conditions

Considering that in this study, the length of the converter is 7.5 meters, the number of 15 points is considered in the calculations. In other words, the length of each element is 0.5 meters. In order to make sure that the number of points is sufficient, the calculations for the number of points less and more i.e. 5 and 30 points have also been done. As it is clear from the Figure (4r), the results for the number of 15 and 30 points are completely coincident, but for 5 points, there is some error in the output of the converter. This shows that the number of 15 points in calculations is sufficient.

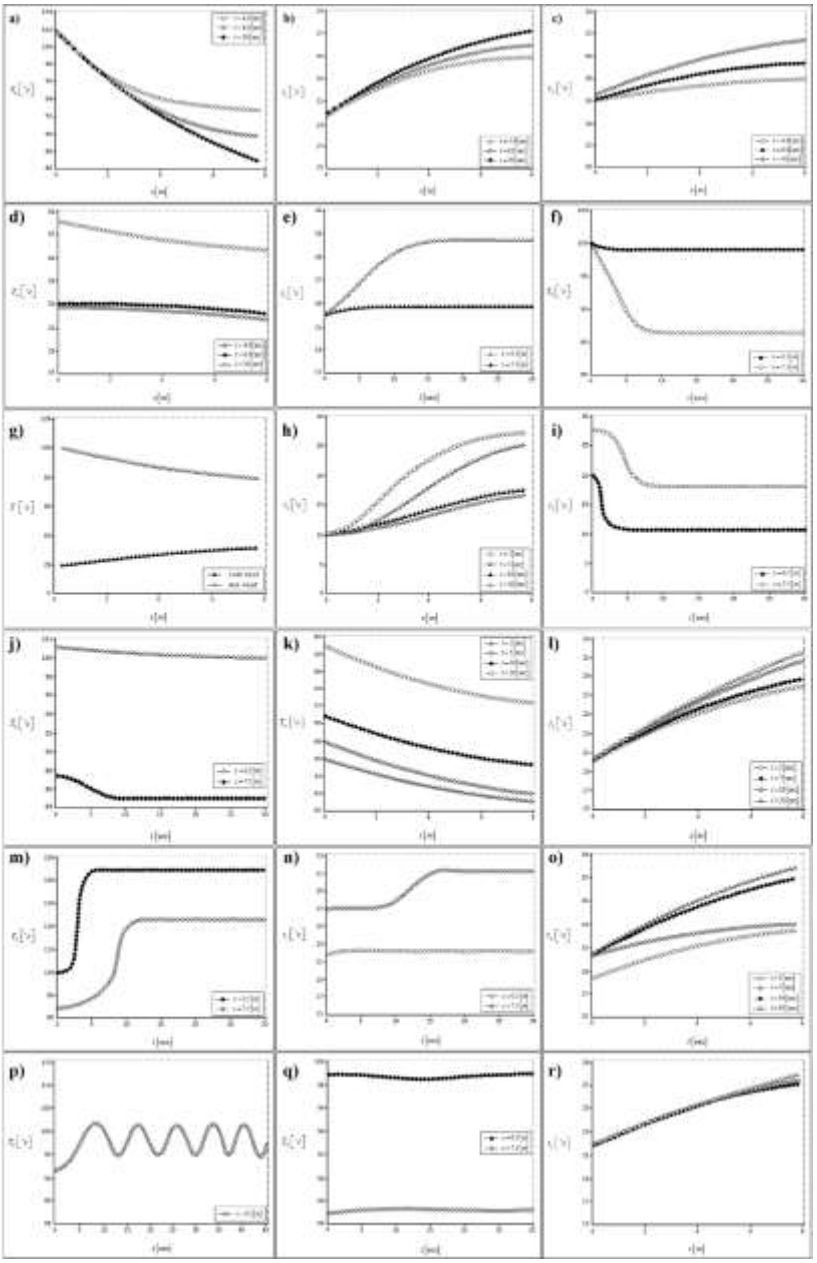

Figure 4. Temperature of hot fluid (a), cold fluid (b), pipe (c), shell (d) in terms of location at different times; temperature of cold

fluid (e), hot fluid (f) and mixture of cold and hot fluid (g) in terms of time; temperature of cold fluid in terms of location at different times for cold fluid stage function (h); temperature of cold fluid (i) and cold fluid (j) and shell (k) in terms of time at the inlet and outlet of the converter and for the phase change of the cold fluid; temperature of cold fluid along the converter in terms of time for change the phase change of hot fluid (l); temperature of hot fluid (m), cold fluid (n) in terms of time at the inlet and outlet of the converter and for the phase change of hot fluid; temperature of the tube in terms of the location at different times for the operation of the hot fluid stage (o); temperature of inlet and outlet hot fluid in terms of time for the operation of sinusoidal conditions (p) and steady state conditions (q).

3.6. Equivalent Electric Circuit

In order to analyze the behavior of converters in an unstable state, they can be equated with an electric circuit including a series of capacitors and resistors. In this work, each fluid or body is simulated by a capacitor and a resistor. In the transient state, according to the energy equation mentioned in the third chapter, the role of heat capacity is determined. Heat capacity appears in the energy equation as the coefficient of the time term of the equation and plays the role of a capacitor in energy storage with discharge. In this work, the behavior of the converter with an electric circuit is simulated as follows (Figure 5).

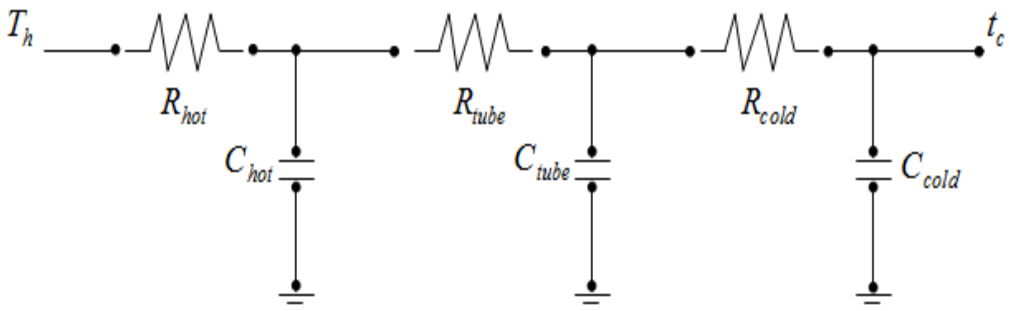

Figure 5. Equivalent electric circuit.

As seen from Figure 5, each area is equalized by a resistor and a capacitor. The temperature difference at the two ends of the circuit is equivalent to the voltage difference, the thermal resistance is equivalent to the electrical resistance, the thermal capacity is equivalent to the capacitor and the thermal flux is equivalent to the current. We know that in the steady state, when the capacitors are full, they practically do not play a role in the response of the circuit and are removed from the circuit. But in the unstable state, when the capacitors are being filled, they create a time delay in reaching the stable state of different areas (internal fluid, external fluid, and walls).

The filling time of a capacitor is five times its time constant, and the time constant of filling or discharging the capacitor is equal to the product of the resistance and the capacity of the capacitor, RC. As a result, the time to reach the stability of the system is a function of the resistance and thermal capacity of the circuit. The values of resistance and capacity of equivalent capacitors are obtained from the following Equations:

$$\boldsymbol{R_{cold}} = \frac{\mathbf{1}}{\boldsymbol{h_1 A_1}} \quad (2)$$

$$\boldsymbol{R_{tube}} = \frac{\boldsymbol{ln\frac{r_2}{r_1}}}{\boldsymbol{2\pi L k_w}} \quad (3)$$

$$\boldsymbol{R_{hot}} = \frac{\mathbf{1}}{\boldsymbol{h_2 A_2}} \quad (4)$$

$$\boldsymbol{C_{cold}} = \boldsymbol{\rho_c V_c\ cP_c} \quad (5)$$

$$\boldsymbol{C_{tube}} = \boldsymbol{\rho_w V_w\ cP_w} \quad (6)$$

$$C_{hot} = \rho_h V_h \, cP_h \quad (7)$$

where V indicates the volume of the area and is obtained from the following Equations:

$$V_c = \pi r_1^2 L \quad (8)$$

$$V_w = \pi M (r_2^2 - r_1^2) L \quad (9)$$

$$V_h = \pi (r_3^2 - M r_2^2) L \quad (10)$$

3.7. Effect of baffle cutting on heat and power transfer coefficients

For the numerical analysis of the tube shell heat exchanger turbulence model algorithm, six variable values of baffle cut 0.25, 0.30, 0.35, 0.40, 0.45, 0.50 have been considered, while the baffle angle is 90 degrees. The speed of the fluid flow in the shell part increases with the reduction of the baffle cut. At the same time, it is clear that the dead areas of the flow gradually decrease due to the increase in the amount of water fluid.

Figure 6a and b shows the effects of baffle cutting on the pressure drop inside the shell and tube exchanger. The pressure drop increases with the decrease of the baffle cut, which corresponds to the change in the flow rate. And in particular, when the baffle cut-off changes from 0.5 to 0.25 at a mass flow rate of m=300 Kg/s, it increases up to 2.7 times. The effects of baffle cutting on the performance of the relationship between the heat transfer rate and power consumption are determined, as shown in Figure 31-5, the heat transfer rate reaches its maximum value at the baffle cut value of 0.45 and 0.4, and when the cut value is at its minimum value equal to 0.25, the amount of consumed power reaches its same state. For example, the heat transfer rate at a power of 100 W increases by 9.8% for a baffle cut of 0.4 compared to a cut of 0.25. Based on the available results, it can be concluded that the baffle cut of 0.45 and 0.4 has the optimal value in comparison with the other six modes.

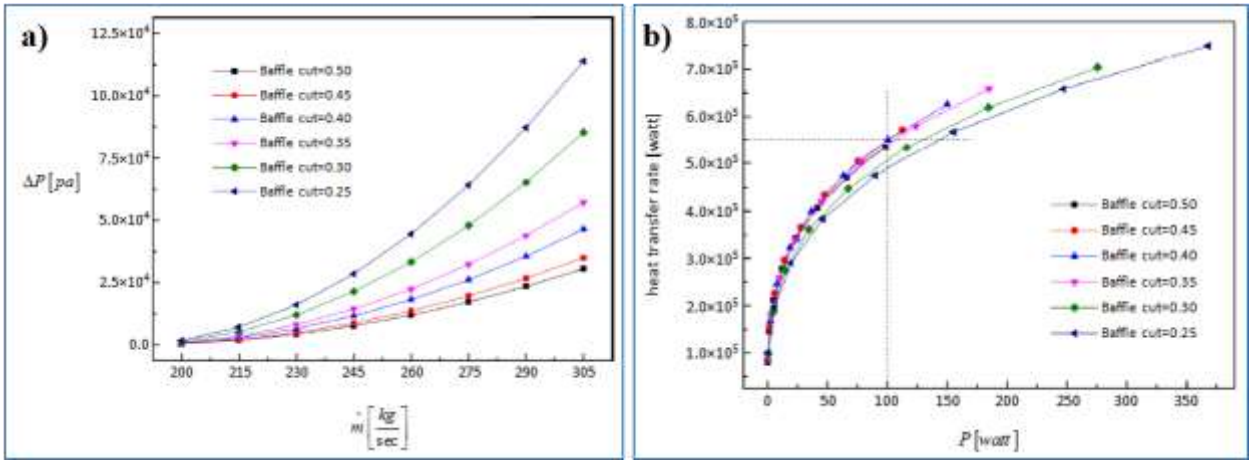

Figure 6. The effect of baffle cutting on pressure drop (a) and heat transfer coefficient (b) inside the shell and tube exchanger.

Thermohydraulic flow contours inside the shell and tube heat exchanger are shown in Figure (7 a-d). The contours of the speed path line for two different flow conditions with the same flow from one side with the number of variable baffles; which show the amount of disturbance during the converter. In Figure (7e), the converter with the number of 6 and 12 baffles for the initial mass flow rate of hot fluid is 200 Kg/s and the mass flow of cold fluid is 244.8 Kg/s. Pressure drop results are improved based on CFD analysis. When the number of baffles reaches 12, the difference decreases to less than 10%. The percentage difference between the number of baffles 6 to 12 is less than 2%.

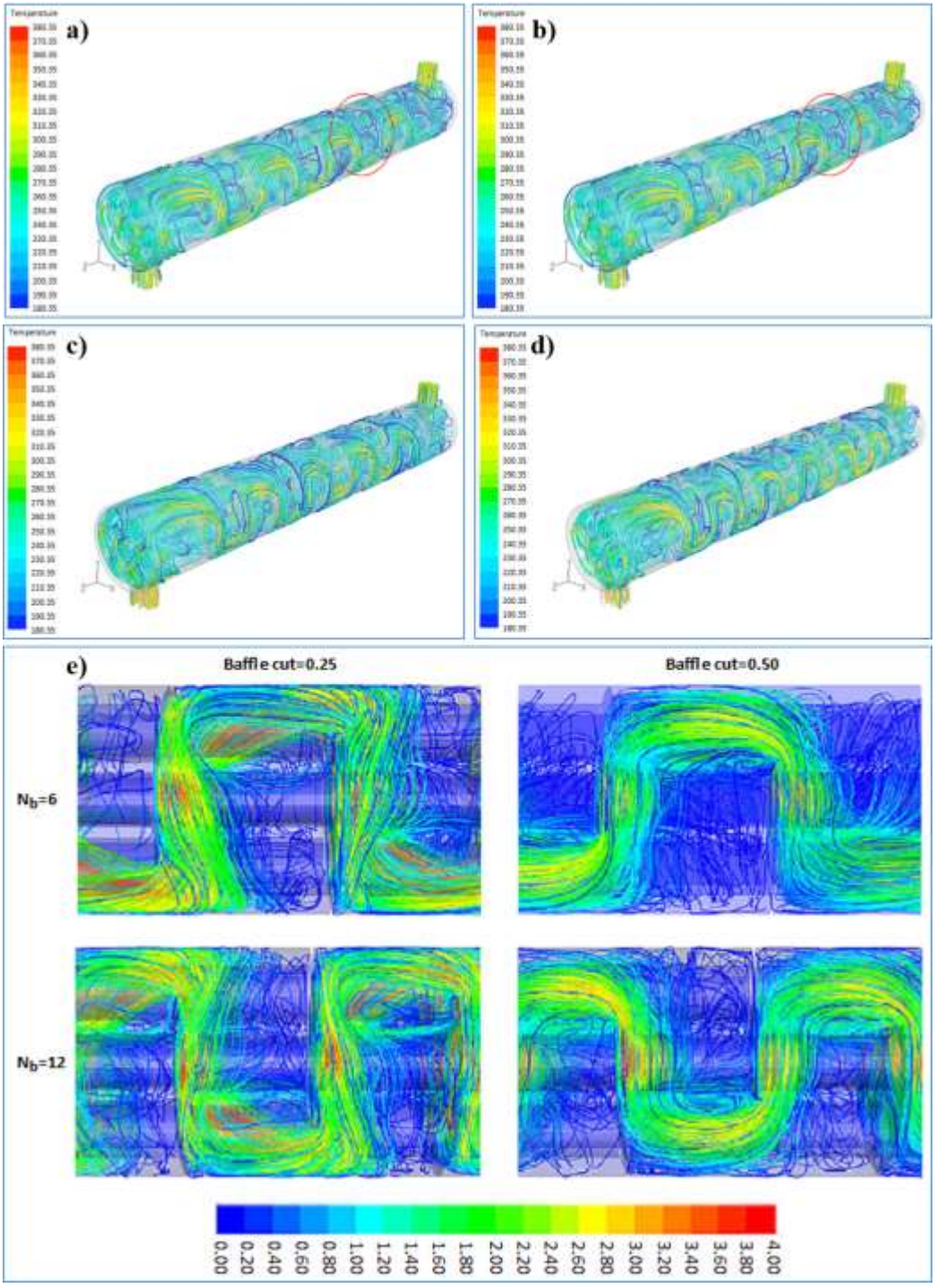

Figure 7. The contour of the velocity line with (a) 6, (b) 8, (c) 10 and (d) 12 baffles, (e) 6 and 12 baffles and taking into account the initial flow rate of hot fluid equal to 200 kg/s and for cold fluid equal to 244.8 kg/s.

By changing the distance and number of our baffles between 6 and 12 and the baffle cut values from 25%, 30%, 35%, 40%, 45%, 50% for shell volume flow rates considering 200 Kg/s to 300 Kg/s, the simulation results are obtained (Table 9). For well-spaced walls, it can be seen that the CFD simulation results give good sinusoidal flow diagram agreement. Also, these results are sensitive to the choice of the baffle cutoff, so that the results have a good convergence in terms of the cutoff of 0.4 and 0.45.

Table9. Analysis results of CFD program based on different distances and number of baffles.

Number Baffle	Mass Flow Rate $[kg/s]$	Shell Side Outlet Temp. $[K]$	Heat Transfer Coeff. $[watt/m^2.K]$	Shell Side Pressure Drop $[Pa]$	Total Heat Transfer Rate $[watt]$
6	$200kg/s$	382.36	3260	6212	96521
	$244.8kg/s$	375.26	4558	9023	100786
8	$200kg/s$	384.85	3389	8055	109115
	$244.8kg/s$	378.27	4870	10780	124780
10	$200kg/s$	385.97	3572	9963	122360
	$244.8kg/s$	379.16	5126	11577	131885
12	$200kg/s$	386.45	3894	10831	124189
	$244.8kg/s$	380.22	5782	13947	146550

CONCLUSIONS

Heat exchangers are very useful equipment in a wide range of industries. Therefore, the analysis of the internal flow in them, both in terms of momentum and thermal, is very important. The shell and tube heat exchanger has a very important effect in industrial processes, therefore, in this research, the dynamic modeling of the shell and tube heat exchanger has been considered. A heat exchanger is modeled to solve the flow and temperature field. At first, based on the finite volume method, the heat exchanger is divided into several parts in the longitudinal direction, then energy conservation is applied to the volume components of different domains (hot and cold fluid - inner and outer walls), and the result is four sets of differential equations for the volume components There are four components of analysis. Three turbulence models have been tested for first and second order discretization using two different mesh densities. Then the obtained equations are written in the form of state space and finally analyzed in the environment. The results obtained from the analysis of the model in different modes are as follows.

At the same time, this model has a faster calculation speed than similar ones, which can reduce the calculation time. The effects of different parameters on the internal conditions of the converter have been simulated. Various changes including the type of fluids, pipes, heat transfer coefficients, mass flow rate and other things have been analyzed.

At the beginning, the condition where the input mass rate of one of the fluxes changes stepwise has been evaluated and it has been shown that the speed of reaching the steady state for one of the fluxes is considered by increasing the mass rate of the fluxes. With these changes, the stable and unstable conditions in the converter undergo changes. Conditions where fluids have a high heat capacity, their thermal inertia is greater and they reach a stable state more slowly. But another point is the heat transfer coefficient, in viscous fluids, the heat transfer coefficient will be low due to the high viscosity. In this case, the temperature changes also decrease in proportion to the reduction of the heat transfer coefficient. Meanwhile, the Reynolds number and the Parantel number affect the heat transfer rate, and the role of the Reynolds number is greater than that of the Parantel number. The effects of increasing the displacement heat transfer coefficient around the exchanger are very small in the free displacement range, although it was not very effective in forced displacement flows.

From the CFD simulation results, for the tube with constant wall temperature and shell inlet, the heat transfer coefficient on the shell side, the pressure drop values and the heat transfer rate are obtained. In another part, the effect of changes in the type of pipes on the dynamic state of the converter is presented. It has been shown that the stabilization time of the fluid temperature has a direct relationship with the heat capacity of the pipes. In this way, as

the heat capacity of the pipes increases, the time for the temperature profiles of the fluids to stabilize will increase.

In the other part, temperature inputs with step shape have been investigated. In this section, it is shown that if there is a disturbance in the temperature of one of the streams, the other stream will also be affected, but its response will be with a time delay and a smaller amplitude. In this research, it has also been shown that a fluid that undergoes disturbance reaches a stable state much faster than another fluid.

From the numerical results, it can be concluded that the performance of the tubular heat exchanger with spiral walls is better than that of segmental walls. So that the changes of the heat transfer coefficient are high for the low angles of the helix. Also, the pressure drop increases with the increase of the angle of inclination of the baffle. Finally, the intermittent temperature input has been investigated. In these cases, it has been shown that if the temperature of one of the fluxes fluctuates intermittently, the other flux will also fluctuate with the same frequency but with a smaller time delay and amplitude, which is also in harmony with the theoretical issues.

REFERENCES

[1] J. Zhang, X. Zhu, M. E. Mondejar, F. J. R. Haglind, S. E. Reviews, "A review of heat transfer enhancement techniques in plate heat exchangers," vol. 101, no. pp. 305-328, 2019, doi:

[2] Q. Xiao, K. Yang, M. Wu, J. Pan, J. Xu, H. J. A. T. E. Wang, "Complexity evolution quantification of bubble pattern in a gas-liquid mixing system for direct-contact heat transfer," vol. 138, no. pp. 832-839, 2018, doi:

[3] P. M. Kumar, V. J. M. T. P. Hariprasath, "A review on triple tube heat exchangers," vol. 21, no. pp. 584-587, 2020, doi:

[4] S. Genić, B. Jaćimović, A. J. A. T. E. Petrovic, "A novel method for combined entropy generation and economic optimization of counter-current and co-current heat exchangers," vol. 136, no. pp. 327-334, 2018, doi:

[5] C. K. Mangrulkar, A. S. Dhoble, S. Chamoli, A. Gupta, V. B. J. R. Gawande, S. E. Reviews, "Recent advancement in heat transfer and fluid flow characteristics in cross flow heat exchangers," vol. 113, no. pp. 109220, 2019, doi:

[6] Y. Lei, Y. Li, S. Jing, C. Song, Y. Lyu, F. J. A. T. E. Wang, "Design and performance analysis of the novel shell-and-tube heat exchangers with louver baffles," vol. 125, no. pp. 870-879, 2017, doi:

[7] E. Zanchini, A. J. G. Jahanbin, "Effects of the temperature distribution on the thermal resistance of double u-tube borehole heat exchangers," vol. 71, no. pp. 46-54, 2018, doi:

[8] B. Gao, B. Liu, J. Dong, J. Shi. Application of Sub-Modeling in the Finite Element Analysis of a Large Fixed Tubesheet Heat Exchanger. Pressure Vessels and Piping Conference: American Society of Mechanical Engineers; 2017. p. V03AT03A064.

[9] G. Zhu, C. Qian, M. J. J. o. P. V. T. Xue, "A New Analytical Theory for the Strength Calculation of the Two Different Tubesheets in Floating-Head Heat Exchangers," vol. 142, no. 5, pp. 051304, 2020, doi:

[10] M. R. Sarmasti Emami, A. J. N. S. v. M. S. I. Gholami, "An analytical study on the effect of fouling and water quality on corrosion of kettle heat exchanger," vol. no. pp. 2019, doi:

[11] A. L. Costa, E. M. J. A. t. e. Queiroz, "Design optimization of shell-and-tube heat exchangers," vol. 28, no. 14-15, pp. 1798-1805, 2008, doi:

[12] A. A. A. Arani, R. J. A. T. E. Moradi, "Shell and tube heat exchanger optimization using new baffle and tube configuration," vol. 157, no. pp. 113736, 2019, doi:

[13] A. A. Tahery, S. Khalilarya, S. J. H. T. A. R. Jafarmadar, "Effectively designed shell-tube heat exchangers considering cost minimization and energy management," vol. 46, no. 8, pp. 1488-1498, 2017, doi:

[14] R. Amano, B. Sundén. Computational fluid dynamics and heat transfer: emerging topics: WIT Press, 2011.

[15] S. Logtenberg, M. Nijemeisland, A. G. J. C. E. S. Dixon, "Computational fluid dynamics simulations of fluid flow and heat transfer at the wall–particle contact points in a fixed-bed reactor," vol. 54, no. 13-14, pp. 2433-2439, 1999, doi:

[16] H. Afrianto, M. R. Tanshen, B. Munkhbayar, U. T. Suryo, H. Chung, H. J. I. J. o. H. Jeong, et al., "A numerical investigation on LNG flow and heat transfer characteristic in heat exchanger," vol. 68, no. pp. 110-118, 2014, doi:

[17] O. D. Hernández-Parra, A. Plana-Fattori, G. Alvarez, F.-T. Ndoye, H. Benkhelifa, D. J. J. o. F. E. Flick, "Modeling flow and heat transfer in a scraped surface heat exchanger during the production of sorbet," vol. 221, no. pp. 54-69, 2018, doi:

[18] C. Yu, S. Qin, B. Chai, S. Huang, Y. J. E. Liu, "The Effect of Compressible Flow on Heat Transfer Performance of Heat Exchanger by Computational Fluid Dynamics (CFD) Simulation," vol. 21, no. 9, pp. 829, 2019, doi:

[19] B. Gürel, V. R. Akkaya, M. Göltaş, Ç. N. Şen, O. V. Güler, M. İ. Koşar, et al., "Investigation on flow and heat transfer of compact brazed plate heat exchanger with lung pattern," vol. 175, no. pp. 115309, 2020, doi:

[20] U. Zahid, A. Hanan, T. Feroze, S. J. A. J. o. M. E. Khan, "Analysis of the performance optimisation parameters of shell and tube heat exchanger using CFD," vol. no. pp. 1-14, 2021, doi:

[21] A. Moraveji, D. J. I. J. o. H. Toghraie, M. Transfer, "Computational fluid dynamics simulation of heat transfer and fluid flow characteristics in a vortex tube by considering the various parameters," vol. 113, no. pp. 432-443, 2017, doi:

[22] H. Md Lokman, R. Bel Fdhila, U. Sand, J. Engdahl, E. Dahlquist, H. Li. CFD Modeling of Real Scale Slab Reheating Furnace. 12th International

Conference on Heat Transfer, Fluid Mechanics and Thermodynamics, Costa del Sol, Spain, 11-13 July, 20162016.

[23] A. G. Kanaris, A. A. Mouza, S. V. J. C. E. Paras, T. I. C. P. E. P. Engineering-Biotechnology, "Flow and heat transfer prediction in a corrugated plate heat exchanger using a CFD code," vol. 29, no. 8, pp. 923-930, 2006, doi:

[24] M. S. Shadloo, G. Oger, D. Le Touzé, "Smoothed particle hydrodynamics method for fluid flows, towards industrial applications: Motivations, current state, and challenges," Computers & Fluids, vol. 136, no. pp. 11-34, 2016, doi:

[25] W. Yang, J. Zeng, D. Zhang, "Contrasting phase field method and pairwise force smoothed particle hydrodynamics method in simulating multiphase flow through fracture-vug medium," Journal of Natural Gas Science and Engineering, vol. 81, no. pp. 103424, 2020, doi:

[26] A. Amicarelli, S. Manenti, R. Albano, G. Agate, M. Paggi, L. Longoni, et al., "SPHERA v. 9.0. 0: A Computational Fluid Dynamics research code, based on the Smoothed Particle Hydrodynamics mesh-less method," Computer Physics Communications, vol. 250, no. pp. 107157, 2020, doi:

[27] A. Eitzlmayr, J. Khinast, "Co-rotating twin-screw extruders: Detailed analysis of conveying elements based on smoothed particle hydrodynamics. Part 1: Hydrodynamics," Chemical engineering science, vol. 134, no. pp. 861-879, 2015, doi:

DOI: https://doi.org/10.15379/ijmst.v10i3.1672